

The Trans-Iron Galactic Element Recorder for the International Space Station (TIGERISS)

Brian F. Rauch^{†,a,*} and Wolfgang V. Zober^a for the TIGERISS Collaboration

^a*Department of Physics and McDonnell Center for the Space Sciences, Washington University,
St. Louis, MO 63130 USA*

E-mail: brauch@physics.wustl.edu

TIGERISS is an ultra-heavy Galactic cosmic ray (UHGCR) detector awarded under the second round of the NASA Astrophysics Pioneers Program, planned to launch in 2026 and which will measure the abundances of every element from ${}_5\text{B}$ to ${}_{82}\text{Pb}$ relative to ${}_{26}\text{Fe}$ with kinetic energies over 350 MeV/nucleon. TIGERISS is the successor to the TIGER and SuperTIGER long-duration balloon instruments incorporating silicon strip detectors in place of scintillation detectors and scintillating fibers and using silicon photomultipliers (SiPM) instead of photomultiplier tubes (PMT). These new detector components have been tested at CERN/SPS beam runs and will provide TIGERISS with high fidelity charge assignment with $\sigma_Z \leq 0.25$. Instrument configurations for available ISS external attachment accommodations on the JAXA JEM-EF and the ESA Columbus Laboratory are being studied for site selection at the end of the formulation phase. The TIGERISS geometry factor depends on attachment location (~ 1 to $1.6 \text{ m}^2\text{sr}$), but in one year the threshold instrument would obtain statistics comparable to the current SuperTIGER UHGCR data set while expanding measurements to higher and lower atomic numbers. These measurements will be cleaner than SuperTIGER's, as they will not require corrections for atmospheric interactions and scintillator saturation effects, and will give the first single-element resolution measurements of elements above ${}_{56}\text{Ba}$. Extended observations will test models of UHGCR origins and cover elements produced in s-process and r-process neutron capture nucleosynthesis, adding to the multi-messenger effort to determine the relative contributions of supernova (SN) and Neutron Star Merger (NSM) events to r-process nucleosynthesis.

38th International Cosmic Ray Conference (ICRC2023)
26 July - 3 August, 2023
Nagoya, Japan



*Speaker

[†]TIGERISS supported by NASA under cooperative agreement 80NSSC22M0299, the McDonnell Center for the Space Sciences, and the Peggy and Steve Fossett Foundation

1. Introduction

The Trans-Iron Galactic Element Recorder for the International Space Station (TIGERISS) has a planned launch in 2026 and will provide the best data set yet for ultra-heavy Galactic cosmic rays (UHGCRs). This data set will enable TIGERISS to address questions about the grand cycle of matter in the Galaxy, including the nature of the astrophysical reservoirs of nuclei at the Galactic cosmic-ray (GCR) sources and the mechanisms by which nuclei are removed from the reservoirs and injected into the cosmic-ray accelerators. It will also allow TIGERISS to search for sources of r-process neutron capture synthesis of the heavier elements. Previous GCR measurements point to a source drawn primarily from older interstellar media (ISM) with fresh nucleosynthetic products of younger stars mixed in and acceleration by shock waves from stellar deaths. The GCRs help energize Galactic magnetic fields and feed back into the process of new star formation, as depicted in Fig. 1. This picture has been pieced together over many years from evidence gleaned from measurements of elemental and isotopic composition, energy spectra, and gamma rays emitted in cosmic-ray interactions with the ISM.

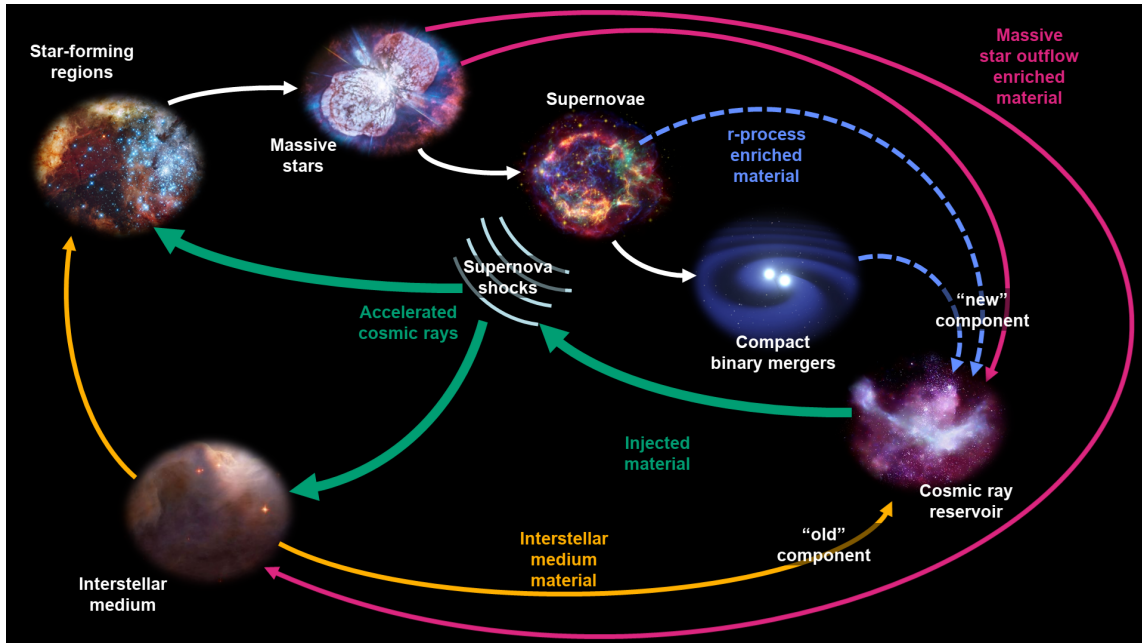


Figure 1: Cycle of matter in the Galaxy. Star forming regions create massive stars that inject matter into the interstellar medium via stellar wind and supernova shocks. Many of the heaviest nuclei are produced in the most energetic processes: supernova and NSM.

For many years cosmic-ray acceleration and the r-process neutron capture nucleosynthesis of the heavier elements in the cycle shown in Fig. 1 were thought to occur predominantly if not exclusively in supernovae. More recent multi-messenger observations of kilonovae involving gravitational wave [1] and broader electromagnetic spectral observations [2] have provided strong evidence supporting the model of binary neutron star merger nucleosynthesis of the heaviest r-process elements. The first single-element resolution UHGCR measurements above $_{40}\text{Zr}$ by SuperTIGER indicate that something is missing from the GCR source (GCRS) model with a major contribution from OB associations and preferential acceleration of elements condensed on dust grains [3–6]. TIGERISS

will investigate the elemental composition of the heavier UHGCRs with unprecedented resolution to address these scientific questions, which are discussed in more detail in [7].

2. TIGERISS Instrument

The proposed TIGERISS location on the International Space Station (ISS) was the Japan Aerospace Exploration Agency (JAXA) Japanese Experiment Module (JEM) “Kibo” Exposed Facility Unit 10 (EFU10), but this is now expected to be occupied in 2026. We have been required to study payload configurations for all possible external attachment locations, and we are developing models for JEM-EFU6 and EFU7 and the European Space Agency (ESA) Columbus Laboratory external payload Starboard Overhead X-Direction (SOX) location. None of the zenith facing National Aeronautics and Space Administration (NASA) EXpedite the PROcessing of Experiments to the Space Station (ExPRESS) Logistics Carrier (ELC) locations are expected to be available. A technical model of the Columbus SOX configuration (1.28 m² sr) is shown in Fig. 2a, and that for a JEM-EF standard payload configuration (1.19 m² sr) is shown in Fig. 2b. The JEM-EF wide version (1.83 m² sr) would require a waiver from JAXA, and would be 1 m wide and 0.8 m tall instead of 0.8 m wide and 1 m tall, having a 20 cm greater payload and instrument width.

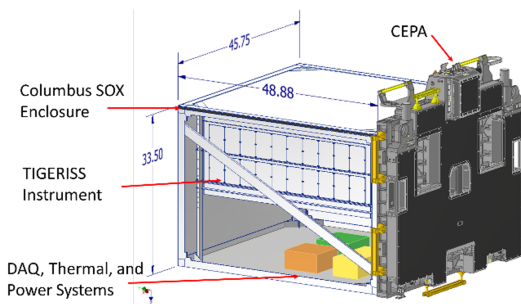


Figure 2(a): Columbus SOX TIGERISS payload technical model.

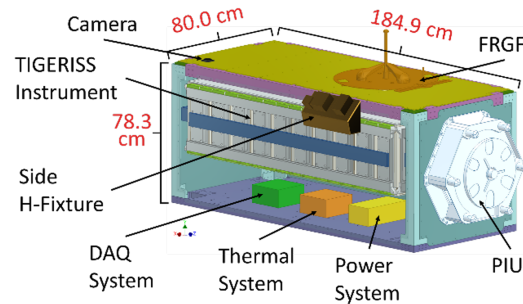


Figure 2(b): JEM-EF standard TIGERISS payload technical model.

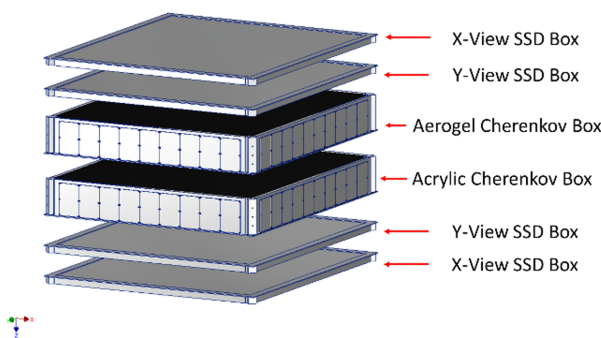


Figure 2(c): Expanded view of the standard TIGERISS payload technical model.

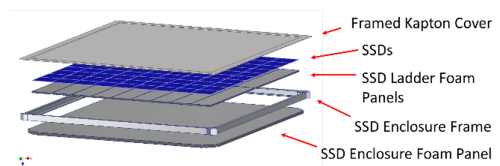


Figure 2(d): SSD expanded view.

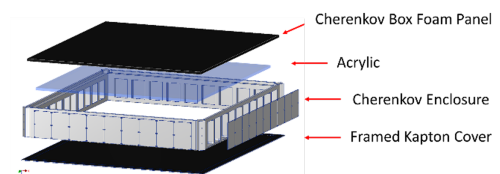


Figure 2(e): Cherenkov detector expanded view.

An expanded view of the TIGERISS SOX model is shown in Fig. 2c. TIGERISS will use three basic detector subsystems to unambiguously measure the charge of all GCRs from ₅B to ₈₂Pb with energies greater than ~0.2 GeV/nucleon. TIGERISS uses crossed pairs of SSD layers at the top and

POS (ICRC2023) 171

bottom of the instrument stack to measure both particle trajectory and ionization energy deposits (dE/dx), replacing the scintillating optical fiber hodoscopes and scintillator detectors used in the TIGER family of stratospheric balloon-borne instruments. An expanded view of a SSD module is shown in Fig. 2d. Two Cherenkov detectors measure nuclear charge (Z) and velocity (β): C0 with a silica aerogel radiator over C1 with an acrylic radiator, with an expanded view of the acrylic detector shown in Fig. 2e.

CERN beam tests of SSD detectors have demonstrated single element resolution ($\sigma_Q \leq 0.24$) down to ~ 200 MeV/nucleon for $Z \geq 5$ [8]. These detectors are a significant improvement on the scintillators used in TIGER/SuperTIGER [9, 10] in both resolution and linearity of signal response with Z , as they do not suffer from saturation effects. The charge assignment method using the multiple SSD dE/dx measurements independently and with Cherenkov signals above their thresholds complements the acrylic Cherenkov ($n=1.49$, $\beta > 0.67$, $KE \geq 325$ MeV/nucleon) versus aerogel Cherenkov ($n=1.05$, $\beta > 0.95$, $KE \geq 2.12$ GeV/nucleon) technique successfully demonstrated on TIGER/SuperTIGER for energies above the aerogel threshold [9, 10]. TIGERISS will be capable of measuring elements to the end of the periodic table, but statistics will limit it to $Z \sim 82$ for any foreseeable exposure duration.

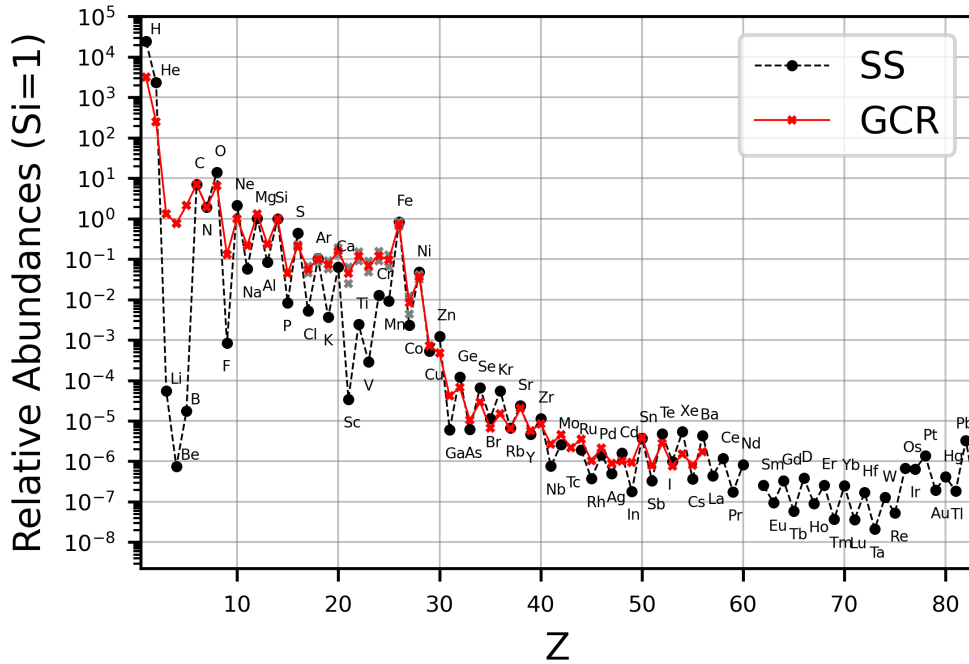


Figure 3: Solar System (SS) [11] and Galactic cosmic-ray (GCR) relative abundances at 2 GeV/nuc. The red line depicts average GCR data, sourced for $1 \leq Z \leq 2$ from [12], $Z=3$ from [13], $4 \leq Z \leq 28$ from [14], and $16 \leq Z \leq 56$ from [3] normalized to ^{14}Si . Grey dots depict overlapping measurements from [14] and [3].

3. Science Objectives

3.1 Ultra-Heavy Galactic Cosmic Rays

The GCRs and the Solar System (SS) represent two directly measurable samples of Galactic matter, with the few million year old GCRs being far younger than the ~ 4.6 billion year old SS

sample of the Galactic ISM. A comparison of the relative abundances of GCRs with energies of ~ 2 GeV/nucleon [5, 9, 12–14] to those of SS [11] from ${}^1\text{H}$ to ${}_{56}\text{Zr}$ normalized to ${}_{14}\text{Si} = 1$ is shown in Fig. 3. In the GCRs ${}_{26}\text{Fe}$ is $\sim 5 \times 10^3$ times less abundant than ${}^1\text{H}$, and the UHGCRs are in turn $\sim 10^5$ times less abundant than ${}_{26}\text{Fe}$. The major differences between the GCR and SS abundances seen below ${}_{26}\text{Fe}$ are generally understood to arise from elemental acceleration efficiencies of the GCR and nuclear fragmentation between the GCRS and detection.

Figure 3 shows GCR abundances through ${}_{56}\text{Ba}$ measurements with single-element resolution, with the UHGCRs from SuperTIGER [5]. UHGCR measurements through ${}_{40}\text{Zr}$ by TIGER [9], SuperTIGER [10] and ACE-CRIS [15] together with ACE-CRIS isotopic measurements (${}^{22}_{10}\text{Ne}$ [16], ${}_{26}\text{Fe}$ [17]) suggest that the GCRS is enhanced in material produced in massive stars ejected by solar winds and in supernovae. Figure 4a shows that for GCR observations up to ${}_{40}\text{Zr}$ corrected for propagation effects to GCRS abundances the refractory elements that are more readily embedded in interstellar dust grains are preferentially accelerated over volatile elements, and that injection into the GCRs for both refractory and volatile elements appears to follow a charge dependence consistent with their grain sputtering cross sections ($\propto Z^{2/3}$) [18]. This suggests that a significant fraction of the cosmic rays originate in OB associations where material from earlier generations of massive stars ($\sim 20\%$) mixes with ISM ($\sim 80\%$) and is accelerated by subsequent supernovae.

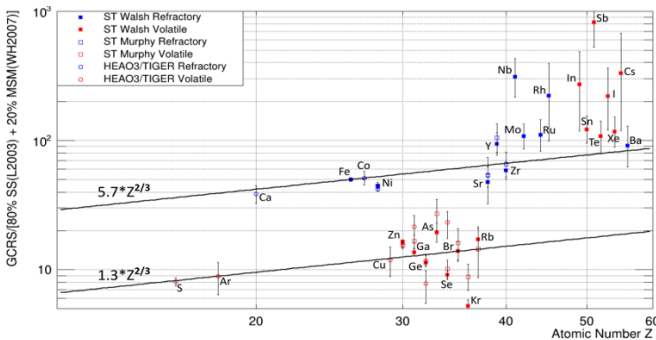


Figure 4(a): SuperTIGER results through ${}_{56}\text{Ba}$ showing that the existing model is insufficient for elements above ${}_{40}\text{Zn}$.

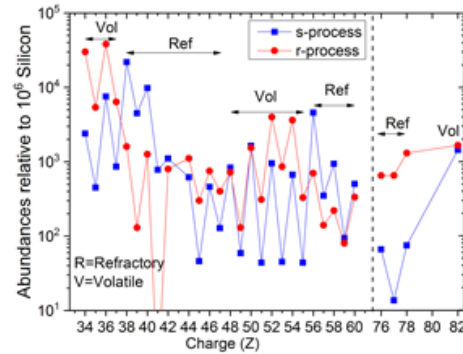


Figure 4(b): Model of s- and r-process composition showing refractory and volatile elements.

More recent SuperTIGER analysis extended the UHGCR measurements from the first flight up to ${}_{56}\text{Ba}$ [3, 4, 6], showing that above ${}_{40}\text{Zr}$ volatile elements are enhanced to roughly the same degree as the refractories. The breakdown of the OB association GCRS model for UHGCR elements where the s-process no longer dominates over the r-process suggests the possibility of another source component other than ISM and fresh massive star material, such as neutron star merger (NSM) material. The breakdown in the preferential acceleration of refractory elements may also in part result from this material being old enough that the volatile elements have had sufficient time and appropriate conditions to condense onto dust grains at a level comparable to the refractory elements.

TIGERISS observations will help determine the relative amounts of nucleosynthesis by s- and r-process neutron capture in the UHGCRs and help determine the relative contributions of massive stars and NSMs to r-process nucleosynthesis. Figure 4b gives a model deconvolution of the two main neutron-capture processes as a function of atomic number and also shows which elements are volatile and refractory. TIGERISS will disentangle the contributions from GCRS components

and preferential acceleration by measuring UHGCR abundances through ^{82}Pb . In only one year significant measurements will be made of the more abundant dominant s-process (^{50}Sn and ^{56}Ba) and r-process elements (^{52}Te , ^{54}Xe). Three of these are volatile (^{50}Sn , ^{52}Te and ^{54}Xe) and only one is refractory (^{56}Ba), which will allow us to disentangle the impact of acceleration efficiency to determine the relative contributions of the r- and s-process to the GCRs in the ^{50}Sn - ^{56}Ba group.

3.2 Energy Spectra

TIGERISS will be able to measure the energy spectra of the more abundant elements between ^5B to ^{28}Ni from above the ~ 200 MeV/nucleon detection threshold to where the silica aerogel Cherenkov signal plateaus, near $\beta = 1$ above ~ 10 GeV/nucleon. These measurements will complement those by other instruments, including AMS-02 and CALET already on the ISS, and the ACE-CRIS and DAMPE satellite instruments. The comparatively large area of TIGERISS will make it a sensitive probe for temporally variant spectral features that could arise from phenomena like microquasars.

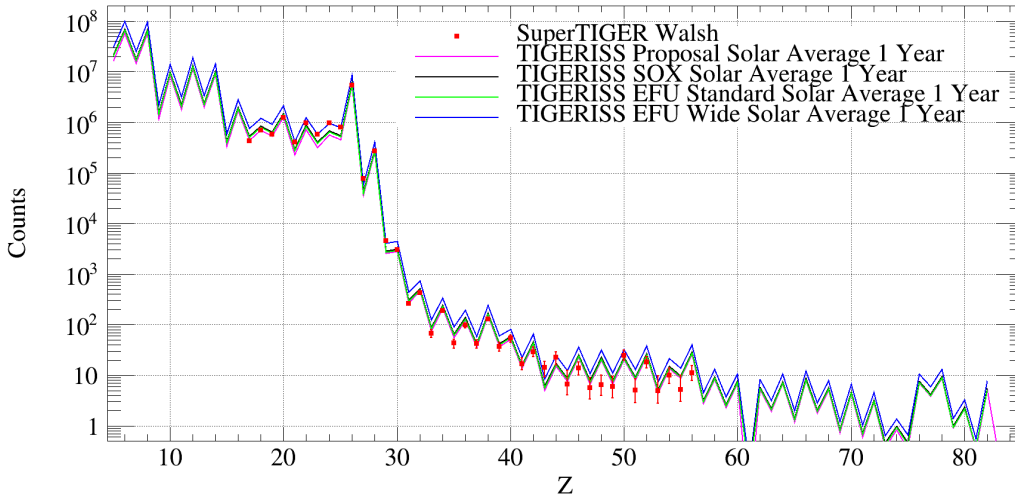


Figure 5: Predicted abundances measured by TIGERISS after 1 year of operation [19] to those measured by SuperTIGER over its 55 day long-duration-balloon flight [3–6].

4. Predicted TIGERISS Observations

4.1 One Year Statistics for Astrophysics Pioneers

TIGERISS measurements in the ~ 1 year it will have on the ISS under the original NASA Astrophysics Pioneers Program award will address important science goals. Figure 5 gives predicted one year TIGERISS measurements for the proposal JEM-EF model (pink), Columbus SOX (black), current JEM-EF standard model (green), and JEM-EF wide model (blue) configurations [19] compared with those from the first SuperTIGER flight (red) [3–6]. The level of solar modulation does not have a strong impact on the TIGERISS UHGCR measurements, and the expected one-year statistics are comparable to or better than those of SuperTIGER with superior charge resolution. The TIGERISS predictions between ^{40}Zr and ^{60}Nd are based on the assumed 20% odd/80%

even splitting of charge pairs measured by HEAO-3-C2 [20], which agree reasonably with the SuperTIGER measurements, and abundances of elements in charge groups above ${}_{60}\text{Nd}$ are scaled by SS abundances. Major differences include unstable ${}_{43}\text{Tc}$ enhanced at balloon altitudes by secondary production and the elements around ${}_{48}\text{Cd}$ where the transition between high- and low-gain measurements in SuperTIGER makes their comparatively low measured values suspect. TIGERISS measurements through ${}_{56}\text{Ba}$ will check the SuperTIGER results, while also probing the r- and s-process contributions to the UHGCR in the ${}_{50}\text{Sn}$ - ${}_{56}\text{Ba}$ group.

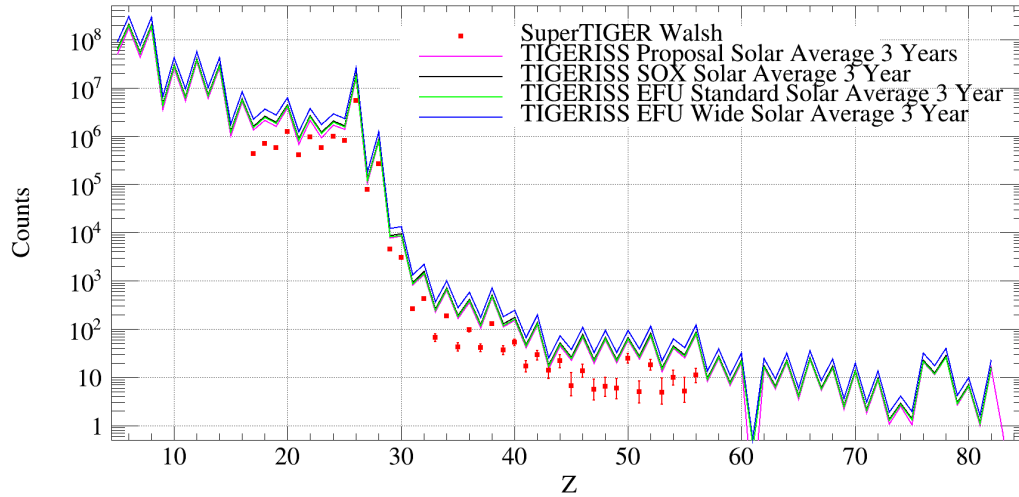


Figure 6: Predicted abundances measured by TIGERISS after 3 years of operation [19] compared to those measured by SuperTIGER over its 55 day long-duration-balloon flight [3–6].

4.2 Statistics from Extended Observations

Provided TIGERISS delivers as expected in its first year we would propose extended operations to increase its scientific return. Figure 6 shows the TIGERISS statistics expected under average solar modulation conditions from three years of observations for the same payload configurations in Fig. 5 for one year. This would take TIGERISS to around the end of the currently planned ISS operations, and the increased statistics would provide much more significant measurements of the abundances of the heaviest UHGCR nuclei, including ${}_{76}\text{Os}$, ${}_{78}\text{Pt}$ and ${}_{82}\text{Pb}$.

5. Conclusions

The TIGERISS instrument combining silicon strip and Cherenkov detectors will be capable of measuring all of the GCRs from ${}_{5}\text{B}$ to ${}_{82}\text{Pb}$ with single element resolution, which will probe the GCRs and the mechanism that injects this material into the accelerator. In one year of measurements under the Astrophysics Pioneers Program, TIGERISS will verify the SuperTIGER results with different systematics and double the total statistics of the UHGCR measurements that conflict with the leading GCRS model. TIGERISS will also make the first preliminary single-element UHGCR measurements from ${}_{56}\text{Ba}$ to ${}_{82}\text{Pb}$ while probing the relative contributions of r- and s-process neutron capture sources to the GCRs.

6. References

- [1] B. P. Abbott *et al.*, “Gw170817: Observation of gravitational waves from a binary neutron star inspiral,” *Phys. Rev. Lett.*, vol. 119, p. 161101, Oct 2017.
- [2] B. P. Abbott *et al.*, “Multi-messenger observations of a binary neutron star merger,” *The Astrophysical Journal*, vol. 848, p. L12, oct 2017.
- [3] N. E. Walsh, *SuperTIGER Elemental Abundances for the Charge Range $41 \leq Z \leq 56$* . PhD thesis, Washington University in St. Louis, 2020.
- [4] N. E. Walsh *et al.*, “SuperTIGER Abundances of Galactic Cosmic Rays for the Atomic Number (Z) Interval 30 to 56,” in *Proceedings of 37th International Cosmic Ray Conference — PoS(ICRC2021)*, vol. 395, p. 118, 2021.
- [5] N. E. Walsh *et al.*, “SuperTIGER instrument abundances of galactic cosmic rays for the charge interval $41 \leq Z \leq 56$,” *Advances in Space Research*, vol. 70, pp. 2666–2673, Nov. 2022.
- [6] N. E. Walsh, “SuperTIGER Abundances of Galactic Cosmic Rays for the Atomic Number (Z) Interval 40 to 56,” in *Proceedings of 38th International Cosmic Ray Conference — PoS(ICRC2023)*, vol. 444, p. 053, 2023.
- [7] W. V. Zober, B. F. Rauch, *et al.*, “Science Objectives and Goals of the TIGERISS mission,” in *Proceedings of 38th International Cosmic Ray Conference — PoS(ICRC2023)*, vol. 444, p. 144, 2023.
- [8] J. F. Krizmanic *et al.*, “HNX/SuperTIGER Silicon Strip Detector Response to Nuclei in Lead Primary and Fragmented Test Beams,” in *36th International Cosmic Ray Conference (ICRC2019)*, vol. 36 of *International Cosmic Ray Conference*, p. 94, July 2019.
- [9] B. F. Rauch *et al.*, “Cosmic Ray Origin in OB Associations and Preferential Acceleration of Refractory Elements: Evidence from Abundances of Elements ^{26}Fe through ^{34}Se ,” *The Astrophysical Journal*, vol. 697, no. 2, pp. 2083–2088, 2009.
- [10] R. P. Murphy *et al.*, “Galactic Cosmic Rays Origins and OB Associations: Evidence from SuperTIGER Observations of Elements ^{26}Fe through ^{40}Zr ,” *The Astrophysical Journal*, vol. 831, no. 2, p. 148, 2016.
- [11] K. Lodders, “Solar System Abundances and Condensation Temperatures of the Elements,” *The Astrophysical Journal*, vol. 519, pp. 1220–1247, 2003.
- [12] T. Sanuki *et al.*, “Precise Measurement of Cosmic-Ray Proton and Helium Spectra with the BESS Spectrometer,” *The Astrophysical Journal*, vol. 545, no. 2, pp. 1135–1142, 2000.
- [13] M. Aguilar *et al.*, “Isotopic Composition of Light Nuclei in Cosmic Rays: Results from AMS-01,” *The Astrophysical Journal*, vol. 736, p. 105, Aug. 2011.
- [14] J. J. Engelmann *et al.*, “Charge Composition and Energy Spectra of Cosmic-Ray Nuclei for Elements from Be to Ni. Results from HEAO-3-C2,” *Astronomy & Astrophysics*, vol. 233, pp. 96–111, 1990.
- [15] W. R. Binns *et al.*, “Elemental Source Composition Measurements and the Origin of Galactic Cosmic Rays,” in *36th International Cosmic Ray Conference (ICRC2019)*, vol. 36 of *International Cosmic Ray Conference*, p. 36, July 2019.
- [16] J. C. Higdon and R. E. Lingenfelter, “OB Associations, Supernova-Generated Superbubbles, and the Source of Cosmic Rays,” *The Astrophysical Journal*, vol. 628, pp. 738–749, 2005.
- [17] W. R. Binns *et al.*, “Observation of the ^{60}Fe nucleosynthesis-clock isotope in galactic cosmic rays,” *Science*, vol. 352, pp. 677–680, May 2016.
- [18] R. E. Lingenfelter, “The Origin of Cosmic Rays: How Their Composition Defines Their Source and Sites and the Process of Their Mixing, Injection, and Acceleration,” *The Astrophysical Journal Supplement Series*, vol. 245, p. 30, 2019.
- [19] B. F. Rauch, W. V. Zober, *et al.*, “Modeling Expected TIGERISS Observations,” in *Proceedings of 38th International Cosmic Ray Conference — PoS(ICRC2023)*, vol. 444, p. 172, 2023.
- [20] W. R. Binns *et al.*, “Abundances of Ultraheavy Elements in the Cosmic Radiation: Results from HEAO 3,” *The Astrophysical Journal*, vol. 346, pp. 997–1009, 1989.

Full Author List: TIGERISS Collaboration

R. F. Borda¹, R. G. Bose², D. L. Braun², J. H. Buckley², J. Calderon³, N. W. Cannady^{1,4,5}, R. M. Caputo⁴, S. Coutu⁶, G. A. de Nolfo⁷, P. Ghosh^{8,4,5}, S. Jones³, C. A. Kierans⁴, J. F. Krizmanic⁴, W. Labrador², L. Lisalda², J. V. Martins¹, M. P. McPherson⁹, E. Meyer¹, J. G. Mitchell⁷, J. W. Mitchell⁴, S. I. Mognet⁶, A. Moiseev^{10,4,5}, S. Nutter³, N. E. Osborn², I. M. Pastrana², B. F. Rauch², H. Salmani⁹, M. Sasaki^{10,4,5}, G. E. Simburger², S. Smith⁹, H. A. Tolentino⁹, D. Washington⁶, W. V. Zober²

¹University of Maryland, Baltimore County, ²Department of Physics and McDonnell Center for the Space Sciences, Washington University in St. Louis, ³Northern Kentucky University, ⁴NASA Goddard Space Flight Center, Astrophysics Science Division, ⁵Center for Research and Exploration in Space Sciences and Technology II, ⁶Pennsylvania State University, ⁷NASA Goddard Space Flight Center, Heliophysics Science Division, ⁸Catholic University of America, ⁹Howard University, ¹⁰University of Maryland, College Park